ACS chemical biology

Articles

pubs.acs.org/acschemicalbiology

A Biocompatible *in Vivo* Ligation Reaction and Its Application for Noninvasive Bioluminescent Imaging of Protease Activity in Living Mice

Aurélien Godinat,[†] Hyo Min Park,[‡] Stephen C. Miller,[§] Ke Cheng,[∥] Douglas Hanahan,[∥] Laura E. Sanman,[⊥] Matthew Bogyo,[¶,#] Allen Yu,[‡] Gennady F. Nikitin,[†] Andreas Stahl,[‡] and Elena A. Dubikovskaya*[,†]

[†]Institute of Chemical Sciences and Engineering, Swiss Federal Institute of Technology of Lausanne, LCBIM, CH-1015 Lausanne, Switzerland

[‡]Department of Nutritional Science and Toxicology, University of California Berkeley, Berkeley, California 94720, United States

[§]Department of Biochemistry and Molecular Pharmacology, University of Massachusetts Medical School, Worcester, Massachusetts 01605, United States

[∥]The Swiss Institute for Experimental Cancer Research, School of Life Sciences, Swiss Federal Institute of Technology of Lausanne, CH-1015 Lausanne, Switzerland

[⊥]Department of Chemical and Systems Biology, [¶]Department of Microbiology and Immunology, and [#]Department of Pathology, Stanford University School of Medicine, Stanford, California 94305, United States

Supporting Information

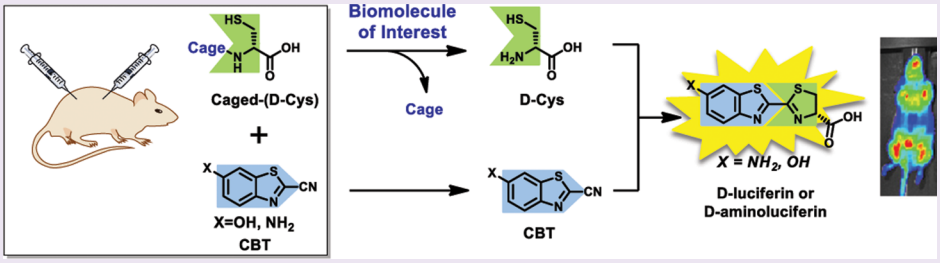

ABSTRACT: The discovery of biocompatible reactions had a tremendous impact on chemical biology, allowing the study of numerous biological processes directly in complex systems. However, despite the fact that multiple biocompatible reactions have been developed in the past decade, very few work well in living mice. Here we report that D-cysteine and 2-cyanobenzothiazoles can selectively react with each other *in vivo* to generate a luciferin substrate for firefly luciferase. The success of this "split luciferin" ligation reaction has important implications for both *in vivo* imaging and biocompatible labeling strategies. First, the production of a luciferin substrate can be visualized in a live mouse by bioluminescence imaging (BLI) and furthermore allows interrogation of targeted tissues using a "caged" luciferin approach. We therefore applied this reaction to the real-time noninvasive imaging of apoptosis associated with caspase 3/7. Caspase-dependent release of free D-cysteine from the caspase 3/7 peptide substrate Asp-Glu-Val-Asp-D-Cys (DEVD-(D-Cys)) allowed selective reaction with 6-amino-2-cyanobenzothiazole (NH_2-CBT) *in vivo* to form 6-amino-D-luciferin with subsequent light emission from luciferase. Importantly, this strategy was found to be superior to the commercially available DEVD-aminoluciferin substrate for imaging of caspase 3/7 activity. Moreover, the split luciferin approach enables the modular construction of bioluminogenic sensors, where either or both reaction partners could be caged to report on multiple biological events. Lastly, the luciferin ligation reaction is 3 orders of magnitude faster than Staudinger ligation, suggesting further applications for both bioluminescence and specific molecular targeting *in vivo*.

In the past decade many biocompatible "click" reactions have been developed and used to study various biological processes in cells and animals.[1] However, only a fraction of these reactions do not require the use of toxic metal catalysts and thus can be used in living cells. These "biocompatible" transformations include copper-free cyclooctyne-type cycloaddition,[2−7] Staudinger ligation,[8−15] alkene-tetrazine reactions,[16−21] and recently reported Pictet-Spengler ligation.[22] Even though studies of various biological processes on the level of live cells have tremendously advanced our understanding of many human pathologies, their great complexity requires tools that allow studies of biochemical processes on the level of the whole organism. Since multiple animal models of various human pathologies have been successfully established,[23−28]

Received: December 28, 2012
Accepted: March 6, 2013
Published: March 6, 2013

   dx.doi.org/10.1021/cb3007314 | *ACS Chem. Biol.* 2013, 8, 987−999

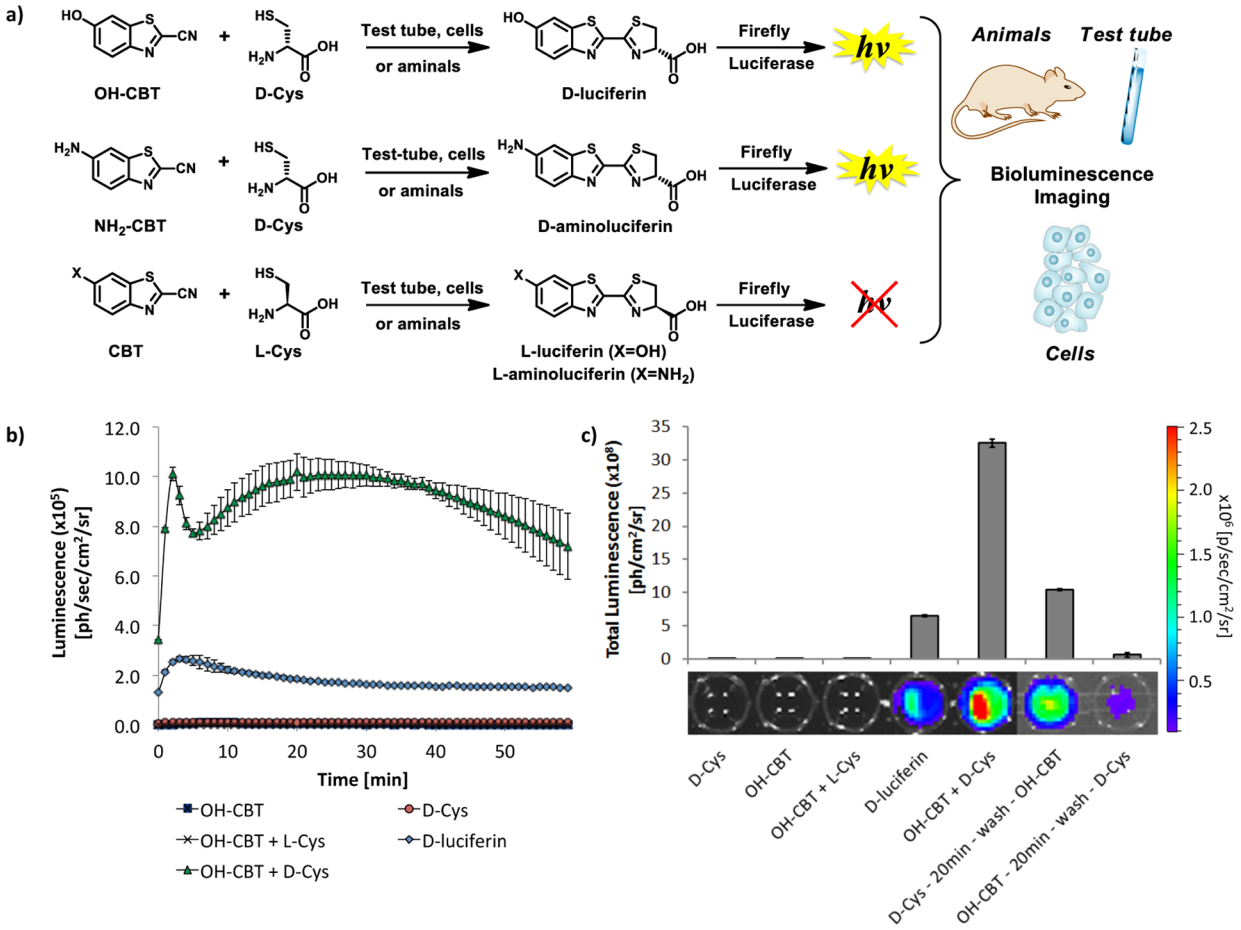

Figure 1. Split luciferin ligation reaction in live cells. (a) Overall schematic of the split luciferin ligation reaction between D- or L-cysteine and hydroxy- or amino-cyanobenzothiazole derivatives (OH-CBT and NH_2-CBT) in various biological environments. (b) Observed bioluminescence produced as a function of time from SKOV3-Luc-D3 live cells, incubated with following reagents: D-cysteine; OH-CBT; OH-CBT plus L-cysteine; OH-CBT plus D-cysteine; and D-luciferin (all at 75 μM in PBS pH = 7.4). Error bars are ± SD for three independent measurements. (c) Total luminescence produced in 1 h from live SKOV3-Luc-D3 cells incubated with corresponding reagents, calculated by integrating the area under corresponding kinetic curves in panel b. SKOV3-Luc-D3 cells were incubated for 1 h with either D-cysteine; OH-CBT; OH-CBT and L-cysteine (added simultaneously); D-luciferin, or OH-CBT and D-cysteine (added simultaneously) at 75 μM in PBS (wells 1−5). Cells first pretreated with D-cysteine for 20 min, followed by wash and 1 h incubation with OH-CBT and cells first pretreated with OH-CBT for 20 min, followed by wash and 1 h incubation with D-cysteine (all at 75 μM in PBS, wells 7−8). Error bars are ± SD for three independent measurements.

development of new biocompatible reactions applicable for studies of biological processes on the level of the whole animal can play a crucial role in biology and medical research.

When the complexity of the system increases from living cells, grown in a Petri dish, to a living animal, many more requirements come into play for successful biocompatible reactions to occur. First, the two components now have to react with each other in the presence of a much more complex biological environment with many more additional active substances, in comparison to the ones found in the cell culture media. Moreover, the organism of a living animal represents a dynamic system, where the reagents could be quickly metabolized by various organs or simply cleared from the circulation before they are able to react. In addition, the reagents and the products of the reaction should be nontoxic to a wide variety of different cells and tissues.

As a result of all these complex requirements, only the Staudinger ligation has been shown to work efficiently in living mice because its reagents possess favorable pharmacokinetics, low toxicity, and the absence of nonspecific binding with other biomolecules in the organism.[1,5,9,11,12,29] Besides its numerous applications in cells, this biocompatible reaction has been previously used for metabolic labeling and imaging of glycans.[9,11,30,31] More recently, [4 + 2] tetrazine/*trans*-cyclooctene cycloaddition has also been shown to work in living mice, albeit with the requirement that the tetrazine reagent is bound to a polymeric support to improve its pharmacokinetic properties.[21]

New biocompatible reactions are therefore needed for use in mouse models of human diseases. One reaction of interest is that of D-cysteine with 6-hydroxy-2-cyanobenzothiazole (OH-CBT), first reported by White and co-workers half a century ago as the final step in the synthesis of D-luciferin.[32] More recently, other groups have reported applications of this reaction for the selective labeling of proteins on N-terminal cysteines[33,34] as well as the controlled assembly of polymers in physiological solutions and living cells.[35,36] Notably, the rate of this reaction has been reported to be 3 orders of magnitude faster than Staudinger ligation.[34] Yet, to date this reaction has never been employed in live mice.

The reaction between D-cysteine and CBTs can yield substrates for firefly luciferase and thus has huge potential for

dx.doi.org/10.1021/cb3007314 | ACS Chem. Biol. 2013, 8, 987−999

use in conjunction with bioluminescence imaging (BLI), the most sensitive *in vivo* imaging technique currently available in living animals to date.[37−39] Historically, BLI has been used to track luciferase-expressing cells *in vivo*[40] as well as for the visualization of transcriptional activation in live animals.[40] More recent applications of BLI include probing of molecular signatures of target tissues through the use of caged small molecule luciferin substrates, which are only uncaged by the activity of specific biological molecules. The underlying principle in the design of all of these caged luciferin substrates is based on the fact that luciferins caged on the phenolic oxygen or aryl nitrogen are not capable of light emission.[29,41−43] This concept was used by others for the design of probes to sense enzymatic activities directly in living animals such as those of β-galactosidase,[43] caspases,[44−48] furin,[49] and β-lactamases.[50] Previously we successfully used this approach for real-time imaging and quantification of fatty acids uptake,[41] cell surface glycosylation,[29] hydrogen peroxide fluxes,[42] as well as studies of efficiency of delivery, linker release, and biodistribution of cell-penetrating peptide conjugates.[51] In addtion, we and others recently reported preparation of new red-shifted luciferin derivatives and their corresponding luciferase enzymes for multicolor application of this powerful imaging modality.[52−55]

Here we report that the reaction between D-cysteine and CBTs can efficiently generate luciferins in live cells and in living mice. This "split luciferin" ligation reaction is therefore highly significant for *in vivo* imaging and shows great promise for *in vivo* biocompatible labeling. One of the advantages of this approach is better cell penetration properties of CBT derivatives in comparison to full luciferin scaffolds. In addition, CBT derivatives are much easier to synthesize because they possess significantly higher reactivity and stability in comparison to luciferins,[51,56−58] which are known to be sensitive to light, pH, and oxygen.[59,60] Moreover, since both CBT and D-cysteine moieties can be modified with different caging groups, this split luciferin ligation can facilitate the simultaneous detection of multiple events *in vivo*. For example, the hydroxy or amino group on a CBTs can be caged as a sensor for various biomolecules, as previously described for whole luciferin scaffolds.[29,41−50] At the same time, the amine group on the D-cysteine moiety can be caged as a substrate for proteases including caspases,[44−48] thrombin,[47,61] prostate specific antigen,[62,63] and many others that are known to cleave after defined peptide sequences.[47,64]

Finally, the rapid and robust formation of luciferins in live cells and tissues of living mice suggests that the split luciferin ligation reaction can also be more generally used as an *in vivo* labeling strategy. The rate of reaction is 3 orders of magnitude faster than Staudinger ligation, and the chemistry is compatible with all the classical biocompatible reactions, which involve either azide, alkyne, triphenylphosphine, or tetrazine moieties.[1−21] Thus, we anticipate that this reaction can be used in tandem with existing biocompatible reactions to study even more complex biological processes simultaneously in living cells or animals.

RESULTS AND DISCUSSION

***In Vitro* Formation of D-Luciferin and D-Aminoluciferin in Physiological Solutions.** Since the products of all of the previously reported reactions between CBT and cysteine derivatives contained luciferin-like structures, we first investigated whether OH-CBT and NH_2-CBT could form their respective luciferins directly in a biocompatible environment (Figure 1a). Thus, we incubated NH_2-CBT in buffer containing luciferase and compared the production of light resulting from the NH_2-CBT itself versus additions of either D- or L-cysteine. Importantly, the signal produced from the sample that had both NH_2-CBT and D-cysteine was 10-fold higher than the signals obtained from the samples containing either NH_2-CBT alone or NH_2-CBT plus L-cysteine (Supplementary Figure S1a). We further incubated these reagents in PBS buffer and observed formation of corresponding D-luciferin and D-aminoluciferin using high performance liquid chromatography (HPLC), confirmed by high resolution mass spectrometry (HRMS) (Supplementary Figure S1b,c). These results indicate formation of D-luciferin analogues in physiological buffers, which could directly produce photons of light in the presence of firefly luciferase enzyme.

Kinetic Studies of the Reaction between CBT Derivatives and Cysteine. We next studied the rate of the reaction between CBT derivatives and cysteine under pseudo-first-order conditions, using a standard HPLC assay (Supporting Information).[35] The rate constants for the reactions of OH-CBT and NH_2-CBT with L-cysteine were 3.2 and 2.6 M^{-1} s^{-1}, respectively, which is 3 orders of magnitude faster than those reported for the Staudinger ligation.[8,10,13,15] We further compared these reaction rates to that of a previously reported *N*-succinamidyl CBT derivative[34] (compound **1**, Supplementary Table S1 and Figures S2−4). Under our assay conditions, the rate constant for this compound was 7.1 M^{-1} s^{-1}, which is in relative agreement with the previously published value of 9.1 M^{-1} s^{-1}.[34] The lower reaction rate of NH_2-CBT compared to its less electron-donating succinamide derivative is consistent with mesomeric effects on the reactivity of the nitrile. Thus, we expect that the rate of this reaction with CBT derivatives can be further modulated by the introduction of electron-donating or electron-withdrawing ring substituents and that other electrophilic nitriles can be suitable reaction partners.[65] More detailed investigations into the kinetics of the reaction studies between different CBT derivatives and 1,2-aminothiols are currently ongoing in our laboratories.

Real Time Noninvasive Imaging and Quantification of the Split Luciferin Ligation Reaction in Living Cells. We next investigated whether OH-CBT and NH_2-CBT could form their respective luciferins directly in live cells (Figure 1). Thus, ovarian and breast cancer cells, stably transfected with firefly luciferase (SKOV3-luc-D3 and MDA-MB-231-Luc-D3H2LN), were treated with OH-CBT or NH_2-CBT, followed by imaging with a cooled CCD camera. Consistent with the *in vitro* cell-free results, treatment with either CBT derivative or D-cysteine alone produced only a baseline level of signal. The lack of signal from CBT-treated cells could be explained by the fact that its reaction with natural L-cysteine in the cell would result in the formation of L-luciferin, a compound that does not produce light in the presence of luciferase (Figure 1, Supplementary Figures S5 and S6).[66] Similarly, cells treated with equimolar amounts of both OH-CBT and L-cysteine produced the same background signal as cells treated with OH-CBT alone. In contrast, cells treated with either D-luciferin or D-aminoluciferin produced robust signal that was significantly higher than background (Figure 1, Supplementary Figures S5 and S6).

We next incubated cells with equimolar solutions of OH-CBT or NH_2-CBT and D-cysteine. Remarkably, the amount of light produced by the cells treated with D-cysteine and OH-CBT exceeded the signal from an equivalent amount of D-luciferin by at least a factor of 5 (Figure 1, Supplementary

dx.doi.org/10.1021/cb3007314 | *ACS Chem. Biol.* 2013, 8, 987−999

Figures S5 and S6). For example, incubation of live ovarian cancer cells with a 1:1 ratio of OH-CBT and D-cysteine produced 5-fold more light than incubation with an equimolar amount of D-luciferin (Figure 1). Similarly, a 7-fold enhancement was obtained when the same experiment was repeated in live breast cancer cells (Supplementary Figure S6). The signal produced from the two luciferin precursors was concentration-dependent in both cell lines and increased when increasing amounts of each CBT and D-cysteine were added to cells (Supplementary Figures S5 and S6).

This interesting phenomenon could potentially be explained by differences in cell permeability: CBTs and D-cysteine may have better cell permeability than that of D-luciferin itself. In fact, it was previously reported that D-luciferins have suboptimal penetration properties, which can be improved by making their structures more lipophilic.[52,53]

We speculated that if the hypothesis that the precursors of luciferin possess higher cell penetration abilities is true, a big portion of the reaction should be happening inside the cell. In order to see if this is really the case, we performed an experiment in which the cells were preincubated with one of the reagents, followed by washing. Robust signal was observed in both cases, with higher signal being produced when the cells were first preincubated with D-cysteine, followed by extensive washing and subsequent addition of a CBT (Figure 1c, Supplementary Figure S6b). In fact, only 20 min exposure of the cells to D-cysteine followed by a wash and subsequent addition of OH-CBT, resulted in 30% and 60% of the overall signal produced by the SKOV and MDA cells, respectively, compared to incubation with an equimolar concentration of both of the reagents simultaneously for the same period of time (Figure 1c, Supplementary Figure S6b). In addition, these signals are, respectively, 20% and 400% higher than the signal observed from the SCOV and MDA cells, treated with equimolar concentration of D-luciferin control (Figure 1c, Supplementary Figure S6b).

However, when the same experiment was repeated where the sequence of addition of the reagents was reversed (preincubated with OH-CBT for 20 min, then washed and treated with D-cysteine), less than 10% of overall signal was observed in comparison to the signal resulted from simultaneous addition of both CBT and D-cysteine reagents in both cell lines (Figure 1c, Supplementary Figure S6b).

Lastly, a robust concentration-dependent increase in signal was observed when the cells were treated with increasing amounts of D-cysteine, while the concentration of CBT was kept constant. Importantly, this increase was not due to changes in luciferase activity as no increase in signal production was observed when the control cells were incubated with D-luciferin and increasing concentrations of D-cysteine (Supplementary Figures S7 and S8).

Together, these data suggest that both reagents might have much higher permeation abilities than that of D-luciferin alone or higher stability in physiological environment, which is supported by a significant increase in signal after equimolar addition of the two precursors in comparison to full luciferin controls (Figure 1, Supplementary Figure S5 and S6). Indeed, CBT derivatives are more hydrophobic than luciferins due to lack of carboxylic acid moiety, which could explain their better diffusion through the cell membranes. Moreover, while no specific transporters are known to facilitate penetration of luciferins, D-cysteine could still be a substrate for cysteine transporters, responsible for the uptake of L-cysteine by mammalian cells.[67−70] In addition, better stability of the split luciferin ligation reagents in comparison to that of luciferins[51,56−60] may also play a significant role in increased light output from live cells.

Such excellent signal to background ratio makes this reaction ideal for bioluminescence imaging applications.[36−38] Moreover, the fact that significantly more light was observed from the addition of the two luciferin precursors in comparison to already preformed D-luciferin presents an opportunity for even more sensitive imaging of many biological processes in live cells.

Real Time Noninvasive Imaging and Quantification of Split Luciferin Ligation Reaction in Living Animals. Inspired by exciting data from live cell assays, we next asked whether both of the luciferin precursors can react directly in living animals to form their respective luciferins (Figure 2). In order to be able to visualize the product of the reaction noninvasively in real-time, we used transgenic animals that ubiquitously express luciferase in every cell under the control of the β-actin promoter (FVB-luc+ mice).[71,72]

We first injected the mice with either OH- or NH_2-CBT alone and measured the resulting luminescence emission. Similarly to the results obtained in living cells, only background signal was observed (Figure 2b−d). When we then repeated this experiment with the addition of an equimolar amount of D-cysteine 10 min postinjection with CBTs, a robust signal was obtained only a few minutes after injection, suggesting the relatively fast rate of conversion of the reagents to the full D-luciferin scaffold (Figure 2b). Notably, the signal produced from the animals injected with D-cysteine and NH_2-CBT was 2.4 times higher than the signal from the corresponding OH-CBT precursor (Figure 2c), which is consistent with previously reported data for relative light output between D-aminoluciferin and D-luciferin.[37,53,56,73] Significantly, the split luciferin ligation reagents appear to possess desirable pharmacokinetic properties, supported by the fact that robust signal is observed throughout the body of the living animal shortly after injection of both reagents (Figure 2c).

Optimization Studies of Split Luciferin Ligation Reaction in Living Mice. The total light output produced by the animals injected with D-cysteine and equimolar amounts of OH-CBT and NH_2-CBT was 10% and 17%, respectively, of the overall signal obtained from the D-luciferin injected control group (Figure 2). Interestingly, the opposite trend was observed in cells where the split luciferin reagents produced several fold more light than the corresponding preformed D-luciferin derivatives (Figure 1b,c, Supplementary Figures S5 and S6). This change in the ratio of signal production between live animals and tissue culture cells could be due to reaction with free L-cysteine or N-terminal cysteine residues on proteins, binding to serum proteins, or metabolism in the liver.

Since the experiments in cells demonstrated that increased concentration of D-cysteine led to a significant increase in the overall signal production (Figure 1b,c, Supplementary Figures S5 and S6), we decided to inject the animals with one equivalent of OH-CBT or NH_2-CBT, followed by injection with 10 equiv of D-cysteine. The resulting signal was compared with the light output from injection of a 1:1 ratio of both reagents and increased by 7- and 6-fold for OH-CBT and NH_2-CBT, respectively (Figure 2c,d). Importantly, the total light output from the animals injected with a 1:10 ratio of OH-CBT and D-cysteine produced half of the signal obtained from the D-luciferin control group. Moreover, animals injected with a 1:10

dx.doi.org/10.1021/cb3007314 | ACS Chem. Biol. 2013, 8, 987−999

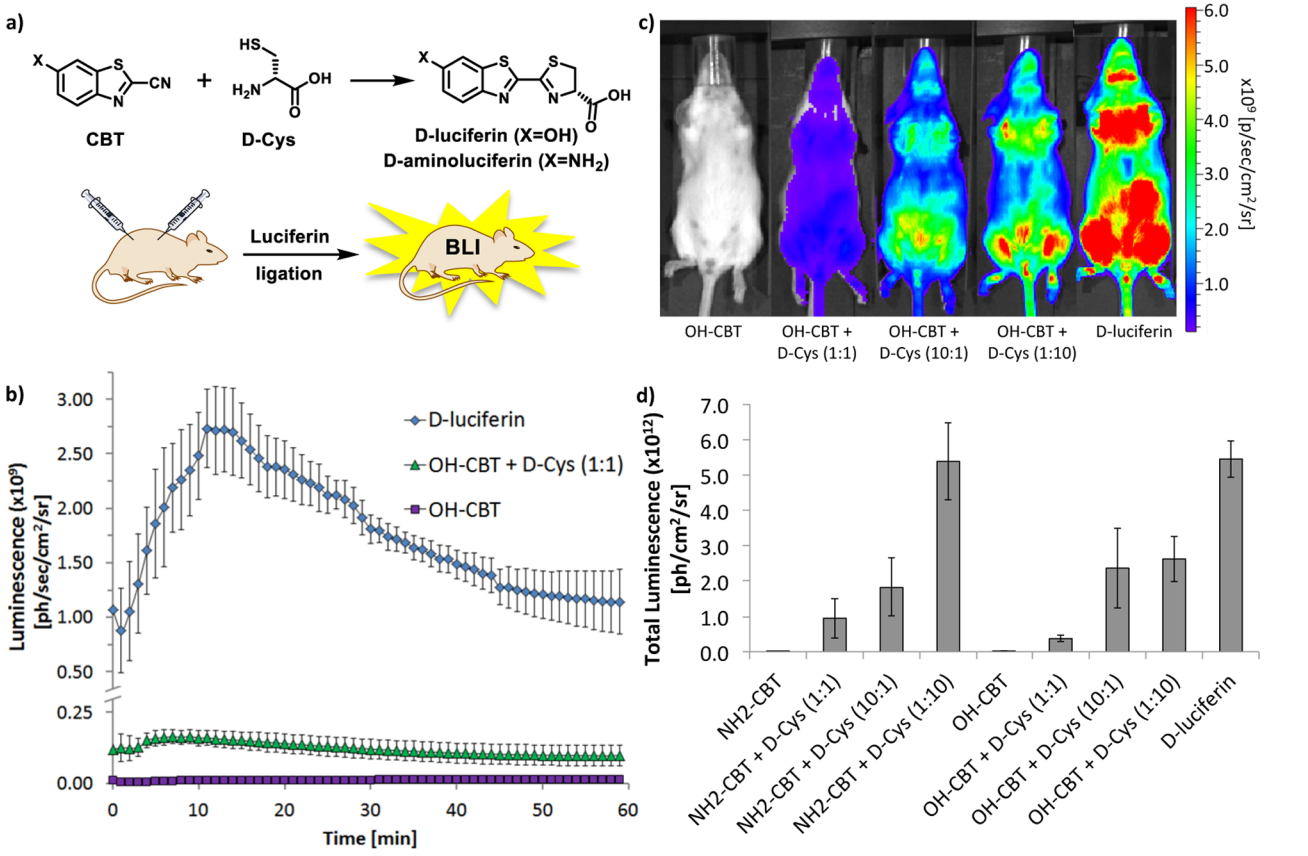

Figure 2. Split luciferin ligation reaction in living mice. (a) Overall schematic of *in situ* formation of D-luciferin or D-aminoluciferin in living transgenic reporter animals. (b) Observed luminescence from luciferase transgenic mice as a function of time after IP injection of D-luciferin; D-cysteine and OH-CBT (equimolar concentrations); OH-CBT. (c) Representative image of mice 15 min postinjection of OH-CBT; OH-CBT and D-cysteine (equimolar concentration); OH-CBT and D-cysteine (10:1 respective concentration ratio); OH-CBT and D-cysteine (1:10 respective concentration ratio); and D-luciferin. (d) Total luminescence over 50 min from resulting bioluminescent signal after IP injection of corresponding reagents (from left to right: NH_2-CBT, NH_2-CBT and D-cysteine in 1:1, 10:1, and 1:10 ratio (bars 1-4); OH-CBT, OH-CBT and D-cysteine in 1:1, 10:1, and 1:10 ratios; and D-luciferin (bars 5-9)). 1 equivalent represents a dose of 0.268 mmol · kg^{-1} in 100 μL of PBS. Error bars are ± SD for five measurements.

ratio of NH_2-CBT and D-cysteine produced an amount of light equivalent to that of the mice injected with the D-luciferin compound (Figure 2c,d). This effect of significant signal enhancement as a result of increased concentrations of D-cysteine was consistent with what was previously observed in cell culture experiments (Figure 1b,c, Supplementary Figures S5 and S6). Interestingly, when the animals were injected with 1 equiv of D-cysteine and 10 equiv of either OH- or NH_2-CBT, significant light enhancement was observed only in case of OH-CBT when compared to equimolar amounts of both the reagents. This observation could be explained by the fact that OH- or NH_2-CBT compounds might have different pharmacokinetic properties when compared directly in living animals.

Comparative Studies of Signal Stability of Split Luciferin Ligation Reaction and D-Luciferin. D-Luciferin, when injected IP, typically produces a sharp peak at around 15 min postinjection with about 3- to 4-fold increase in intensity of the signal, followed by the sudden drop.[74,75] This rapid change in the intensity of the signal observed from D-luciferin injection in animals has been recognized as a real problem in the BLI field for application of this important modality for reliable imaging and quantification of various biological processes.[73,74,76] For example, BLI has been widely used to quantify the size of the tumor burden in xenograft models, in which animals are injected with luciferase-transfected human cancer cells.[77,78] This animal model, in combination with BLI, has been one of the major tools in drug discovery for screening of anticancer drugs in animals.[79,80] However, since the signal from injected luciferin changes significantly over time,[73,75,76] it can be difficult to assess the exact size of the tumor, as the timing of injection and duration of the imaging session can introduce significant errors. Presently, stabilization of the signal from D-luciferin is even more urgent as new 3D imaging BLI technologies become routine and require longer imaging times.[81,82]

Several attempts have been reported to address the problem of D-luciferin signal variability. They include usage of expensive implantable osmotic pumps[73] and repeated substrate injections into the live animals.[75] However, suboptimal results were obtained in both cases, leading to development of new chemically modified D-luciferins, which allow stabilization of the signal. Contag and co-workers have reported the synthesis of a glycine-D-aminoluciferin conjugate, which produced a much more stable signal in comparison to that of D-luciferin alone, although the intensity of the signal was 20−30 times lower than those of D-luciferin or D-aminoluciferin substrates.[75] Similarly, the Denmeade group reported the synthesis of PEGylated luciferin derivatives that result in more stable and prolonged light production from D-luciferin, albeit with a significant reduction in overall light output (Table 1).[76]

dx.doi.org/10.1021/cb3007314 | ACS Chem. Biol. 2013, 8, 987−999

Table 1. Signal Variablility of Luciferin and Its Derivatives upon IP Injection in Living Mice

compounds	signal peak [min]	% of increase before signal peak	% of decrease after signal peak	decrease in intensity compared to unmodified luciferin	synthetic modification/ commercial availability
amino-D-luciferin[a]	10	300	75 in 50 min		no/yes
D-luciferin[a]	5	200	67 in 50 min		no/yes
D-luciferin[b]	15	200	60 in 60 min		no/yes
glycine-D-aminoluciferin[a]	20	c	30 in 60 min	20−30 times	yes/no
PEG-D-aminoluciferin[d]	240	150	60 in 480 min	1.2 times	yes/no
OH-CBT + D-cysteine[b]	15	30	40 in 60 min	10 times	no/yes

[a]Reference 75. [b]Figure 2. [c]The bioluminescence emission from glycine-D-luciferin starts at 0 total photon/s and increases to approximately 2.5 total photon/s in 20 min.[75] [d]Reference 76.

Figure 2b shows the kinetics of light production from free D-luciferin in live transgenic mice in comparison to the signal from equimolar injections of two luciferin ligation precursors. The signal from D-luciferin increased by 200% in the first 15 min to reach the maximum value, followed by 60% decrease from the peak by the 60 min postinjection time point, which comprised a significant change in such a short period of time (Figure 2b). However, the signal from OH-CBT increased by only 30% in the first 15 min followed by 40% decrease from the peak by the 60 min postinjection time point, producing much smaller variability in overall signal. In addition, the light output could be dramatically enhanced by injection of increased amounts of D-cysteine or CBT without significant loss in signal stability (Figure 2c, Supplementary Figure S9). Therefore, the new *in vivo* ligation reaction between CBTs and D-cysteine achieved remarkable stabilization of the signal without any extensive synthetic manipulations (Table 1). Since both CBTs and D-cysteine are commercially available and are several times cheaper than even unmodified D-luciferin itself, this technology offers a simple and powerful tool to overcome existing problems with signal variability from D-luciferins and might be of high potential for the novel 3D imaging applications in the field.

***In Vitro* Imaging of Activity of Thrombin and Caspase 3 Proteases.** Since caged D-luciferin scaffolds have been previously used to quantify and visualize activity of various proteases in living cells and animals,[44−48,56,83−85] we wanted to determine if the *in vivo* reaction between CBTs and D-cysteine can expand or improve this exciting set of tools. The structure of D-cysteine suits itself perfectly for being caged as a substrate for proteases by simply introducing it on to the end of a protease-specific sequence (Supplementary Movie S1). Importantly, multiple essential mammalian and bacterial proteases are known to cleave after specific N-terminal amino acid sequences.[34,40,86−89] While the synthesis of short peptides is cheap and can be readily performed with the help of the automated peptide synthesizers,[90,91] the synthesis of fully caged luciferin scaffolds involves much more complex and low yielding synthetic procedures.[29,37−39,41−43,46,49,50,52−55,83,92]

The production of caged luciferins is further complicated by the fact that only a few reactions have been reported to work on the full luciferin scaffold. They include TFA deprotection,[56] hydrogenation,[57] and the formation of a carbonate from the phenolic oxygen.[51,58] Moreover, luciferins are known to be inherently more sensitive to light, base, and oxidation.[59,60] This greatly limits the production of a broad variety of caged luciferin scaffolds as bioluminescent sensors. Thus, despite many protease-specific sequences known today, very few of them have been used for BLI in the context of caged luciferins[47,56,93−95] and even fewer of them are commercially available.[47] Since CBTs and cysteine derivatives are easier to manipulate and possess higher intrinsic stabilities to light and pH,[47,51,56−60,64] we reasoned that the use of these precursors might circumvent the significant synthetic challenges posed by caged luciferin scaffolds and therefore significantly expand their applications.

To test the viability of this approach, we choose to work with caspase 3 as well as thrombin protease, which all play important roles in several human pathologies.[96−99] Activation of both caspase 3 and 7 is directly connected to apoptosis,[99,100] which plays a key role in many human pathologies such as cancer and atrophy.[96,97] It has been previously reported that DEVD-containing peptides (Asp-Glu-Val-Asp) are selective substrates for caspase 3/7, with cleavage occurring after the second aspartic acid. A bioluminogenic caspase 3/7 sensor is commercially available, in which aminoluciferin has been introduced at the C-terminus of the DEVD peptide and routinely used to detect general apoptosis activities.[47,56]

Thrombin is another example of clinically relevant protease that plays a key role in many blood coagulation-related reactions that prevent a variety of mammalian organisms from extensive blood loss.[101,102] A thrombin-selective peptide sequence has been previously identified (Gly-Gly-Arg) and utilized in multiple *in vitro* tests to assess activity of the protease.[103,104]

Since both caspases 3 and thrombin are known to cleave at the C-terminal end of their corresponding protease-specific sequence of amino acids, we performed the synthesis of these peptides with the addition of D-cysteine at the C-terminal end to yield L-(Asp-Glu-Val-Asp)-D-Cys (DEVD-(D-Cys)) and L-(Gly-Gly-Arg)-D-Cys (GGR-(D-Cys)), respectively. These peptides were then incubated with increasing concentrations of their corresponding proteases, followed by addition of CBT and luciferase buffers. If the protease were active and could recognize its specific peptide sequence, free D-cysteine would be produced in the course of the reaction. Therefore, addition of CBT and luciferase enzyme would consequently result in significant light production, with more light output from the samples with higher concentration of proteases (Figure 3a,b, Supplementary Figures S10 and S11, Movie S1). The efficacy of the peptide specific cleavage can be estimated by direct comparison of the light output from D-cysteine caged peptide with amount of light produced from equimolar amount of free D-cysteine.

It was encouraging to see that strong bioluminescent signals were indeed observed in all samples of protease-specific peptides incubated with their corresponding proteases and that the signal increased with increasing concentration of protease (Figure 3a-b, Supplementary Figures S10 and S11). For example, concentration-dependent signal was observed

dx.doi.org/10.1021/cb3007314 | ACS Chem. Biol. 2013, 8, 987−999

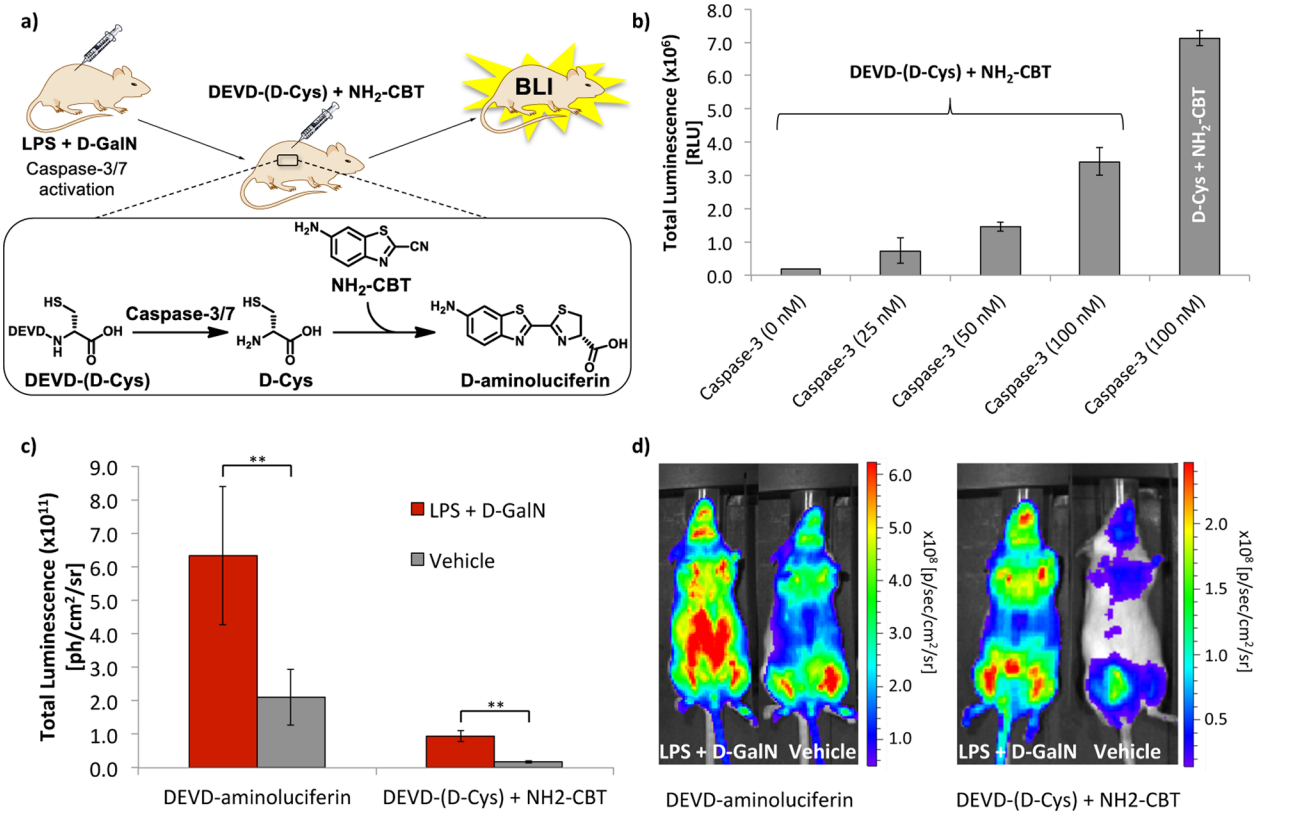

Figure 3. Caspase-3/7 activity imaging using luciferin ligation reaction in living transgenic reporter mice. (a) Overall representation of caspase-3/7 activity imaging with DEVD-(D-Cys) peptide and NH_2-CBT in living animals. (b) Test tube assay of caspase-3 activity imaging with DEVD-(D-Cys) peptide and NH_2-CBT. Total luminescent signal over 2 h from DEVD-(D-Cys) peptide or D-cysteine control (200 μM) after incubation with increasing Caspase-3 concentrations (0, 25, 50, and 100 nM) over 3 h at 37 °C before addition of NH_2-CBT (400 μM) followed by 1 h incubation at 37 °C and subsequent imaging after addition of luciferase buffer. Error bars are ± SD of three measurements. (c) Total luminescence over 1 h from transgenic reporter mice treated with either PBS (control group) or combination of LPS (100 μg/kg in 50 μL of PBS) and D-GalN (267 mg/kg in 50 μL of PBS). Six hours post-treatment, the animals received IP injections of either DEVD-aminoluciferin (34 mg/kg in 100 μL of PBS) or a combination of DEVD-(D-Cys) peptide (22.6 mg/kg in 100 μL of PBS) and NH_2-CBT (6.8 mg/kg in 20 μL of DMSO). Statistical analyses were performed with a two-tailed Student's *t* test. $^{**}P < 0.01$ ($n = 8$ for DEVD-aminoluciferin groups and $n = 4$ for combination of DEVD-(D-Cys) and NH_2-CBT reagents). Error bars are ± SD for 8 and 4 measurements respectively. (d) Representative image of mice treated with LPS and D-GalN or vehicle, 15 min postinjection of DEVD-aminoluciferin or a combination of DEVD-(D-Cys) and NH_2-CBT reagents.

when DEVD-(D-Cys) peptide was incubated with increasing amounts of caspase 3 and subsequently treated with NH_2-CBT-containing luciferase buffer. Importantly, the overall signal produced from DEVD-(D-Cys) peptide incubated with caspase 3 reached 50% of the light output of the signal from the equimolar solution of free D-cysteine control. This experiment shows that DEVD-(D-Cys) peptide remains a good substrate for caspase 3 even upon addition of a D-cysteine amino acid at the C-terminus of the protease-specific sequence (Figure 3b, Supplementary Figure S10).

Similar results were obtained when D-cysteine was caged with the thrombin-selective peptide GGR. A 4-fold increase in BLI signal over background was observed when the GGR-(D-Cys) peptide was incubated with thrombin protease followed by addition of NH_2-CBT, and the signal was protease concentration dependent (Supplementary Figure S11). The outcome of this *in vitro* cell-free experiments demonstrate the feasibility of using a combination of short D-cysteine-caged amino acid sequences with CBTs to study the activity of proteases using bioluminescence.

Real Time Noninvasive Imaging of Caspase 3/7 Activities in Living Animals. Having already established that the luciferin ligation reaction works efficiently in living transgenic reporter animals, we next tested the ability of this approach to quantify the activity of caspase 3/7 in live mice (Figure 3, Supplementary Movie S1). We focused on caspase 3/7 because a well-characterized mouse model of caspase 3/7 activation was previously reported by Promega with a commercially available DEVD-aminoluciferin substrate (Figure 3a).[47,48] In that study, the activity of caspase 3/7 was induced in the liver of FVB-luc+ mice by injecting the animals with lipopolysaccharide (LPS) and D-galactosamine (d-GalN), followed by injection of the DEVD-aminoluciferin substrate and detection of the resulting light production with a CCD camera (Figure 3a).[48]

We repeated this previously reported experiment using the same animals and DEVD-aminoluciferin substrate as a positive control. FVB-luc+ mice were divided into four groups out of which two were injected with equal amounts of d-GalN and LPS followed by either injection of commercial DEVD-aminoluciferin or combination of our DEVD-(D-Cys) peptide and NH_2-CBT. The other two control groups were injected with PBS and combination of the same imaging reagents. The signals from each d-GalN/LPS treated group were compared to each other and their corresponding PBS controls.

dx.doi.org/10.1021/cb3007314 | ACS Chem. Biol. 2013, 8, 987–999

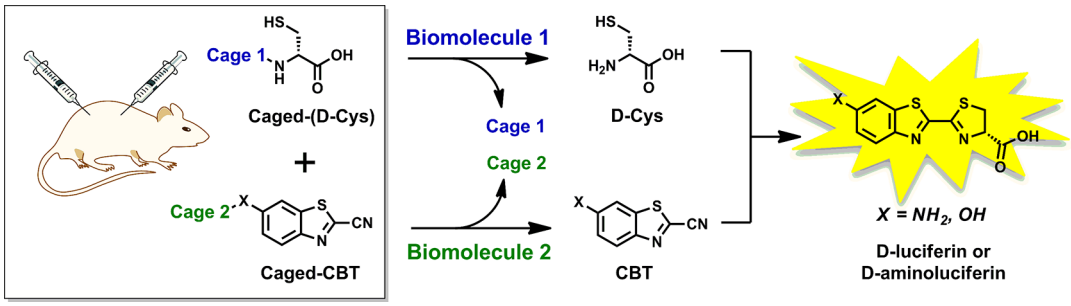

Figure 4. Overall representation of the dual imaging concept for luciferin ligation. Both luciferin ligation precursors could be caged as sensors for two different biomolecules. Only when both become uncaged, D-luciferin or D-aminoluciferin is formed as the result of split luciferin ligation reaction, allowing the production of light by luciferase enzyme.

The data shown in Figure 3c,d and Supplementary Figure S12 indicate that much greater signal was obtained from the two groups of animals treated with d-GalN/LPS in comparison to the control group, treated with PBS. The ratio in average signal we observed between the d-GalN/LPS-treated and control groups of mice injected with commercially available substrate was about 3-fold, which was similar to that previously reported[48] and statistically significant (*P* value: 0.00067, Figure 3c, Supplementary Figure S12a).

At the same time, the ratio between the signals produced from d-GalN/LPS-treated and control groups of mice, injected with combination of DEVD-(D-Cys) peptide and NH_2-CBT, was about 5.2-fold, higher than that of the commercial DEVD-aminoluciferin substrate. Importantly, this difference was also statistically significant (*P* value: 0.00258, Figure 3c, Supplementary Figure S12b). This exciting result could be explained increased efficiency of proteolytic cleavage when it has to cleave between two amino acids, a process happening in nature all the time. However, when the protease has to cleave between the protease-specific sequence and another non-amino acid type of molecule such as aminoluciferin, its efficiency might decrease, even when compared with the cleavage at a D-amino acid.

Inspired by the very positive results in the hepatic model of apoptosis, we next tested whether this method could be widely applied for studies of caspase 3 and 7 activities in other animal models of apoptosis. For that we decided to use xenograft animal models, in which human cancer cells were implanted in immune-deficient mice.

In order to establish a successful animal model, we first tested combinations of several cancer cell lines with different regimens of docetaxel and cisplatin, two commonly used anticancer drugs for treatment of many different type of human cancers.[105−110] Conditions where a majority of cells started to undergo apoptosis upon exposure to the drug were identified for SKOV3-luc-D3 ovarian cancer cells and docetaxel, a drug that has previously been reported to induce apoptosis in this particular cell line (Supplementary Figure S13).[111] Therefore, this cell line, stably transfected with luciferase, was implanted subcutaneously in nude mice, and the tumors were allowed to establish for 6 to 8 weeks.

The animals were then divided in 5 groups (Supplementary Figure S14a): two groups injected with commercial DEVD-aminoluciferin substrate with and without docetaxel treatment, two groups that were injected with a combination of DEVD-(D-Cys) peptide and NH_2-CBT with and without docetaxel treatment, as well as a control group injected with docetaxel and NH_2-CBT alone. To calibrate for the difference in the tumor size, all animals were injected with D-luciferin prior and after the treatment with docetaxel or vehicle alone.

The results from the xenograft animal models, in which apoptosis was induced by treatment with docetaxel anticancer drug, were consistent with the ones obtained in hepatic model of apoptosis (*P* value: 0.00646, Supplementary Figure S14b). However, no significant signal to background ratio was observed from the groups of the animals treated with docetaxel and corresponding vehicle followed by injection of commercial DEVD-aminoluciferin substrate (*P* value: 0.79641). At the same time, a 2-fold increase in signal was observed in mice treated with docetaxel in comparison to the vehicle, followed by imaging with combination of DEVD-(D-Cys) peptide and NH_2-CBT (Supplementary Figure S14b).

Together, these results confirm that the combination of D-cysteine caged peptide sequences and CBTs represents a valuable tool for quantification and imaging of protease activity directly in living animals (Supplementary Movie S1). Since BLI is the most sensitive *in vivo* imaging modality known to date, this tool can be used for screening of activity of multiple proteases as well as identification of their new peptide-specific substrates. Even though we only demonstrated the viability of the split luciferin approach for imaging and quantification of caspase 3/7 activity, many other proteases could be immediately studied using this technique. The examples of such proteases and their specific amino acid sequences include caspase 2 (VDVAD), caspase 6 (VEID), caspase 8 (LETD) and capase 9 (LHTD), caspase 12 (ATAD), dipeptidyl peptidase 4 (GP and VP), and tryptase (PRNK).[34,40,56,86−88] Moreover, this method could also be applied for studies of a wide variety of bacterial, viral, and parasite proteases that are essential for the replication and the spread of infectious diseases.[89] Examples of these proteases include SARS protease (TSAVLQ), caspase-like (nLPnLD), and trypsin-like (LRR) activity of proteasome.[40,86−88] All of these proteases play a very important role in multiple biological processes and are known to cleave at the end of corresponding specific amino acid sequences. On the basis of our new results, this property makes all of them ideal candidates for imaging and quantification of their activities in animal models of disease using the split luciferin approach.

Concluding Remarks. Studies of many biological processes on the level of live cells with the help of biocompatible reactions has tremendously advanced our understanding of basic biology.[1] However, the great complexity of many human pathologies such as cancer, diabetes, and neurodegenerative diseases requires new tools that would allow studies of biological process on the level of the whole organism.

dx.doi.org/10.1021/cb3007314 | *ACS Chem. Biol.* 2013, 8, 987−999

We have found that D-cysteine and CBTs can efficiently react with each other in living cells (Figure 1) and live animals (Figures 2 and 3). This feature makes this reaction very valuable for studies of complex biological processes, because it can be used in tandem with previously known biocompatible reactions. This could be particularly useful in mice, where no applications of biocompatible reactions for studies of several simultaneous events are currently reported, mainly due to the fact that only Staudinger ligation has been shown to work efficiently.[1,5] Moreover, the kinetics of this new *in vivo* split luciferin ligation reaction is 3 orders of magnitude higher than that of Staudinger ligation, opening a wide range of opportunities to use this reaction for studies of fast biological processes that were not feasible before with Staudinger ligation (Supplementary Table S1).

In addition, this split luciferin ligation reaction possesses several other unique features that make it highly useful for a vast variety of exciting biological applications. The two reagents can be specially adapted for bioluminescence imaging, the most sensitive imaging modality known in living animals to date (Figures 1 and 2, Supplemetary Figure S1).[37−39] Since caging of D-cysteine can be combined with caging of amino or hydroxy groups on the CBT moiety, this reaction represents a powerful tool where two or more biological processes can be imaged at once directly in living mice just with this reaction alone (Figure 4). Previously, several probes based on the full luciferin scaffold have been reported for sensitive imaging of multiple biomolecules in live animals, providing a basis for the development of dual imaging approaches.[42,43,46,49,50,83] Remarkably, in cells the signal produced by the split luciferin reagents was several fold higher than the signal from equimolar amounts of already preformed D-luciferin and D-aminoluciferin (Figure 1), providing opportunities for more sensitive imaging of biological processes.

Furthermore, the chemistry of the reagents of this new *in vivo* reaction is well suited for development of novel applications. One of them is real-time imaging of protease activity directly in living animals. In this report, we demonstrate a successful application of this technology for real time noninvasive imaging of caspase 3/7 protease activity in hepatic apoptosis animal models (Figure 3) as well as in tumor xenografts upon treatment with docetaxel (Supplementary Figure S14). When compared to the commercially available DEVD-aminoluciferin substrate,[1,5,42,43,46,49,50,63] the split luciferin ligation reagents had significantly higher signal to background ratio, demonstrating high potential of this new method for sensitive imaging of apoptosis. We further confirmed the applicability of this novel tool for noninvasive studies of activity of other proteases by successfully using this reaction to quantify the activity of thrombin *in vitro* (Supplementary Figure S11, Movie S1).

Even though in this report we have only demonstrated *in vivo* applicability of this new method to quantify and visualize activity of caspase 3/7 protease, the same technique could be used to study activities of other proteases that can use peptide sequences on the N-terminal to the cleavage site,[50,86−89] as well as identify new protease specific peptides associated with various human pathologies. It is noteworthy that the synthesis of short peptide sequences with C-terminal D-cysteine can be easily performed with the help of automated peptide synthesis, which is a widely available and versatile technique.[90,91]

In addition to the new application of the luciferin ligation reaction for imaging activity of biologically relevant molecules, this approach helps remedy an important problem in the BLI field, which is signal instability from D-luciferin and D-aminoluciferin probes. Several-fold signal variation over short period of time from these two most commonly used reagents causes introduction of significant errors for quantification of tumor size or amount of transcriptional activation.[67,69,70] The use of luciferin ligation reaction in animals results in major signal stabilization (30% vs 200% in signal variation in the first 15 min postinjection) without the use of any specially synthesized expensive reagents or implanted osmotic pumps (Figure 2b).[67,69,70] In addition, the intensity of the light output resulting from split luciferin ligation reaction could be significantly increased by injection of higher concentration of D-cysteine (Figure 2, Supplementary Figure S9).

All together, these results demonstrate high potential of this new *in vivo* ligation strategy for the field of chemical biology and medical research. More applications of this exciting technology for noninvasive imaging of biological process are currently being explored in our laboratories. Some of these reagents are already being commercialized by Intrace Medical, Switzerland.

METHODS

General Material and Methods. Caged D-cysteine peptides DEVD-(D-Cys) and GGR-(D-Cys) peptides were custom-made by Protein and Peptide Chemistry Facility (PPCF)−UNIL (University of Lausanne, Switzerland). *N*-Succinamidyl-CBT derivative (compound **1**) was synthesized according to the reported procedure.[35] The rest of the chemicals used in the study were obtained from the following commercial sources and used without further purification. D-Cysteine and NH_2-CBT were purchased from Sigma-Aldrich. L-Cysteine was purchased from Alfa Aesar and OH-CBT was from ABCR GmbH. Luciferase and thrombin protease were purchased from Sigma-Aldrich, ATP was purchased from AppliChem GmbH, and caspase 3 was kindly provided by Dr. Salvesen at Stanford-Burnham Medical Research Institute, CA.[112] Phosphate buffered saline (PBS) was purchased from Life Technologies Corporation. HPLC analysis was performed on Agilent Infinity 1260 HPLC system with either an Agilent Eclipse-XDB-C18 5 μm 4.6 × 250 mm column or Agilent Poroshell 120 EC-C18 2.7 μm 4.6 × 75 mm column using degassed HPLC gradient grade solvent from Fisher Chemicals and Millipore water. The products of the reaction were initially analyzed by Agilent 6120 Quadrupole LC−MS system from Agilent, directly connected to the HPLC. More detailed HRESI-MS measurements were conducted at the EPFL ISIC Mass Spectrometry Service using Micro Mass QTOF Ultima from Waters Corp. Millipore water was used for sample preparation of all *in vitro*, cellular, and animal assays. Only HPLC grade organic solvents were used for all *in vitro* and cellular biological assays and were obtained from Fisher Chemicals. Luciferase buffer used to quantify the amount of luciferin formed during incubation was prepared as following: 60 μg mL^{-1} luciferase (Sigma Aldrich) in 0.1 M Tris-HCl pH = 7.4, 2 mM ATP, and 5 mM $MgSO_4$. All *in vitro* and cellular studies were performed in clear bottom black 96-well plates that were purchased from Becton Dickinson and Company (Franklin Lakes, NJ). Spectramax Gemini (Molecular Devices) or IVIS Spectrum camera (PerkinElmer) were used to measure the amount of BLI signal production.

Cellular Experiments. IVIS Spectrum Camera (PerkinElmer) was used for bioluminescent imaging in all cell experiments. SKOV-3-Luc-D3 cells (PerkinElmer) were cultured in McCoy's 5A modified media obtained from Life Technologies Corporation. MDA-MB-231-Luc-D3H2LN cells (PerkinElmer) were cultured in Minimum Essential α Medium (MEM) obtained from Life Technologies Corporation. Both of the media solutions contained 10% FBS, 1% GlutaMAX and 1% penicillin/streptomycin mixture. Cells were passed and plated (1×10^4 cells/well) in a black 96-well plate with clear bottoms (Becton Dickinson and Company). Then, 48 h after the seeding the growth medium was removed, and the cells were first washed with 200 μL of

dx.doi.org/10.1021/cb3007314 | *ACS Chem. Biol.* 2013, 8, 987−999

PBS, followed by incubation for 5 min with 100 μL solution of D-cysteine or L-cysteine in PBS (150, 15, or 1.5 μM) or PBS alone (control). After a second addition of 100 μL solutions of OH-CBT, NH_2-CBT, or D-luciferin in PBS (150, 15, or 1.5 μM), the cells were immediately placed in the IVIS Spectrum, and the plate was imaged for the duration of 1 h with one image acquired every minute. Observed BLI signal was quantified using region-of-interest (ROI) analysis available on Living Image software (PerkinElmer).

Bioluminescent Caspase-3 Assay with DEVD-(D-Cys) Peptide and Amino-CBT. Caspase-3 was purified and characterized following the reported procedure (kindly provided by Dr. Salvesen at Stanford University, CA).[111] Different concentration solutions of caspase-3 (50, 100, and 200 nM) were prepared in caspase buffer (100 mM HEPES pH 7.4, 0.1% (w/v) CHAPS, 1 mM EDTA, 10 mM DTT, 1% (w/v) sucrose) and were aliquoted in a 96 well-plate (50 μL caspase-3 solution/well). The plate was incubated at 37 °C for 15 min in order to preactivate the caspase. Followed preactivation, 50 μL of a 800 μM DEVD-(D-Cys) solution or 50 μL of a 800 μM D-Cys solution in caspase buffer was added in each well and the plate was incubated at 37 °C for 3 h. After the incubation, 100 μL of a 400 μM solution of NH_2-CBT in MeOH was added to each well and the plate was incubated for another 1 h at 37 °C. Luciferase buffer (60 μg mL^{-1} luciferase in 0.1 M Tris-HCl, 2 mM ATP, 5 mM $MgSO_4$) was freshly prepared and aliquoted in a second 96-well plate (115 μL/well). Five μL of the resulting caspase-3 containing solutions was quickly added to luciferase buffer immediately before reading bioluminescence emission using a Spectramax M5 (Molecular Devices). Bioluminescence signal from the plate was measured every 5 min with 500 ms integration time for the duration of 2 h.

Animals. FVB-luc+ transgenic animals[72] (full abbreviation: FVB-Tg(CAG-luc,-GFP)L2G85Chco/J) mice were kindly provided by the laboratory of Prof. Christopher Contag at Stanford University, rederived at UC Davis, and bred at UC Berkeley. The breeding colony was housed in groups of 4−5 mice according to their age and gender with free access to food and water at 22 °C with regular light-dark cycle. All studies were approved and performed according to the guidelines of the Animal Care and Use Committee of the University of California, Berkeley.

Animal Experiments in FVB-luc+ Mice. IVIS Spectrum Camera (PerkinElmer) was used for BLI imaging in all animal experiments, and the resulting data were processed using Living Image software (PerkinElmer). All solutions were prepared in sterile DMSO obtained from Sigma-Aldrich and PBS purchased from Life Technologies Corporation. Prior to injection and during the imaging procedure mice were anesthetized by inhalation of isoflurane (Phoenix), that was premixed with medical grade oxygen purchased from Praxair. To study split luciferin ligation reaction in living female FVB-luc+ mice, the animals were IP injected with either OH-CBT (5 mice per group); NH_2-CBT (5 mice per group); D-cysteine and OH-CBT in equimolar concentrations (1:1) (5 mice per group); D-cysteine and NH_2-CBT in equimolar concentrations (1:1) (5 mice per group); D-cysteine and OH-CBT in 1:10 ratio (5 mice per group); D-cysteine and NH_2-CBT in 1:10 ratio (5 mice per group); and D-luciferin (5 mice per group). All injections were done at 1 equiv of 0.267 mmol kg^{-1} concentration in either 100 μL of PBS for D-cysteine or D-luciferin and 20 μL DMSO for OH-CBT or NH_2-CBT. The time period of 3 min between IP injection of D-cysteine and CBT derivatives was respected and the animals were imaged right after the second injection with CBT. The animals injected with D-luciferin were imaged right after the injection with the compound.

Real Time Noninvasive Imaging of Caspase 3/7 Activities in FVB-luc+ Mice. Female FVB-luc+ mice (4 mice per group) were anesthetized with isoflurane and injected IP with either lipopolysaccharides (LPS) purchased from Sigma-Aldrich at concentrations of 100 μg kg^{-1} in 50 μL of PBS followed by injections of D-(+)-galactosamine hydrochloride (D-GalN) obtained from AppliChem GmbH at concentrations of 267 mg kg^{-1} in 50 μL of PBS. The control group of mice was injected with 100 μL of PBS (vehicle along). Six hours after injection with combination of LPS and D-GalN or vehicle along (PBS), mice were treated IP with either DEVD-(D-Cys) peptide (22.6 mg kg^{-1} in 100 μL of PBS) plus 6-amino-2-cyanobenzothiazole (NH_2-CBT, 6.8 mg kg^{-1} in 20 μL of DMSO) or commercial DEVD-aminoluciferin substrate (34 mg kg^{-1} in 100 μL of PBS) and imaged. A time period of 10 min between injections of DEVD-D-Cys and NH_2-CBT was respected. The mice were imaged using IVIS Spectrum and bioluminescence images were obtained every minute during the period of 1 h.

■ ASSOCIATED CONTENT

Ⓢ Supporting Information

Supplementary figures. This material is available free of charge via the Internet at http://pubs.acs.org.

■ AUTHOR INFORMATION

Corresponding Author

*E-mail: elena.dubikovskaya@epfl.ch.

Notes

The authors declare no competing financial interest.

■ ACKNOWLEDGMENTS

This work was supported by the grants from Neva Foundation to E.A.D. and National Institutes of Health grants R01DK089202-01A1and R01DK066336-08 to A.S., R01EB013270 to S.C.M., and R01EB05011 to M.B. We thank PerkinElmer (Alameda, CA) for kindly providing us with SKOV3-Luc-D3 and MDA-MB-231-Luc-D3H2LN luciferase transfected cell lines.

■ REFERENCES

(1) Sletten, E. M., and Bertozzi, C. R. (2009) Bioorthogonal chemistry: fishing for selectivity in a sea of functionality. *Angew. Chem., Int. Ed. 48*, 6974−6998.

(2) Agard, N. J., Baskin, J. M., Prescher, J. A., Lo, A., and Bertozzi, C. R. (2006) A comparative study of bioorthogonal reactions with azides. *ACS Chem. Biol. 1*, 644−648.

(3) Sletten, E. M., Nakamura, H., Jewett, J. C., and Bertozzi, C. R. (2010) Difluorobenzocyclooctyne: synthesis, reactivity, and stabilization by beta-cyclodextrin. *J. Am. Chem. Soc. 132*, 11799−11805.

(4) Jewett, J. C., Sletten, E. M., and Bertozzi, C. R. (2010) Rapid Cu-free click chemistry with readily synthesized biarylazacyclooctynones. *J. Am. Chem. Soc. 132*, 3688−3690.

(5) Chang, P. V., Prescher, J. A., Sletten, E. M., Baskin, J. M., Miller, I. A., Agard, N. J., Lo, A., and Bertozzi, C. R. (2010) Copper-free click chemistry in living animals. *Proc. Natl. Acad. Sci. U.S.A. 107*, 1821−1826.

(6) Ning, X., Guo, J., Wolfert, M. A., and Boons, G. (2008) Visualizing metabolically labeled glycoconjugates of living cells by copper-free and fast huisgen cycloadditions. *Angew. Chem., Int. Ed. 47*, 2253−2255.

(7) Neves, A. A., Stöckmann, H., Stairs, S., Ireland-Zecchini, H., Brindle, K. M., and Leeper, F. J. (2011) Development and evaluation of new cyclooctynes for cell surface glycan imaging in cancer cells. *Chem. Sci. 2*, 932−936.

(8) Lin, F. L., Hoyt, H. M., van Halbeek, H., Bergman, R. G., and Bertozzi, C. R. (2005) Mechanistic investigation of the staudinger ligation. *J. Am. Chem. Soc. 127*, 2686−2695.

(9) Saxon, E., and Bertozzi, C. R. (2000) Cell surface engineering by a modified Staudinger reaction. *Science 287*, 2007−2010.

(10) Saxon, E., Armstrong, J. I., and Bertozzi, C. R. (2000) A "traceless" Staudinger ligation for the chemoselective synthesis of amide bonds. *Org. Lett. 2*, 2141−2143.

(11) Prescher, J. A., Dube, D. H., and Bertozzi, C. R. (2004) Chemical remodelling of cell surfaces in living animals. *Nature 430*, 873−877.

(12) Dube, D. H., Prescher, J. A., Quang, C. N., and Bertozzi, C. R. (2006) Probing mucin-type O-linked glycosylation in living animals. *Proc. Natl. Acad. Sci. U.S.A. 103*, 4819−4824.
(13) Nilsson, B. L., Kiessling, L. L., and Raines, R. T. (2000) Staudinger ligation: a peptide from a thioester and azide. *Org. Lett. 2*, 1939−1941.
(14) Chang, P. V., Prescher, J. A., Hangauer, M. J., and Bertozzi, C. R. (2007) Imaging cell surface glycans with bioorthogonal chemical reporters. *J. Am. Chem. Soc. 129*, 8400−8401.
(15) Hangauer, M. J., and Bertozzi, C. R. (2008) A FRET-based fluorogenic phosphine for live-cell imaging with the Staudinger ligation. *Angew. Chem., Int. Ed. 47*, 2394−2397.
(16) Devaraj, N. K., Weissleder, R., and Hilderbrand, S. A. (2008) Tetrazine-based cycloadditions: application to pretargeted live cell imaging. *Bioconjugate Chem. 19*, 2297−2299.
(17) Blackman, M. L., Royzen, M., and Fox, J. M. (2008) Tetrazine ligation: fast bioconjugation based on inverse-electron-demand Diels-Alder reactivity. *J. Am. Chem. Soc. 130*, 13518−13519.
(18) Yang, J., Šečkutė, J., Cole, C. M., and Devaraj, N. K. (2012) Live-cell imaging of cyclopropene tags with fluorogenic tetrazine cycloadditions. *Angew. Chem., Int. Ed. 51*, 7476−7479.
(19) Lang, K., Davis, L., Wallace, S., Mahesh, M., Cox, D. J., Blackman, M. L., Fox, J. M., and Chin, J. W. (2012) Genetic Encoding of bicyclononynes and trans-cyclooctenes for site-specific protein labeling in vitro and in live mammalian cells via rapid fluorogenic Diels-Alder reactions. *J. Am. Chem. Soc. 134*, 10317−10320.
(20) Liang, Y., Mackey, J. L., Lopez, S. A., Liu, F., and Houk, K. N. (2012) Control and design of mutual orthogonality in bioorthogonal cycloadditions. *J. Am. Chem. Soc. 134*, 17904−17907.
(21) Devaraj, N. K., Thurber, G. M., Keliher, E. J., Marinelli, B., and Weissleder, R. (2012) Reactive polymer enables efficient in vivo bioorthogonal chemistry. *Proc. Natl. Acad. Sci. U.S.A. 109*, 4762−4767.
(22) Agarwal, P., Van der Weijden, J., Sletten, E. M., Rabuka, D., and Bertozzi, C. R. (2013) A Pictet-Spengler ligation for protein chemical modification. *Proc. Natl. Acad. Sci. U.S.A. 101*, 46−51.
(23) Rogers, A. B. (2012) Gastric Helicobacter spp. in animal models: Pathogenesis and modulation by extragastric coinfections. *Methods Mol. Biol. 921*, 175−188.
(24) Laferla, F. M., and Green, K. N. (2012) Animal models of Alzheimer Disease. *Cold Spring Harb. Perspect. Med. 2*, a006320.
(25) Peters, M., Trembovler, V., Alexandrovich, A., Parnas, M., Birnbaumer, L., Minke, B., and Shohami, E. (2012) Carvacrol together with TRPC1 elimination improve functional recovery after traumatic brain injury in mice. *J. Neurotrauma 29*, 2831−2834.
(26) Langdon, S. P. (2012) Molecular Pathology in Cancer Therapeutics: where are we now and where are we going? Animal modeling of cancer pathology and studying tumor response to therapy. *Curr. Drug Targets 13*, 1535−1547.
(27) Fedele, M., Gualillo, O., and Vecchione, A. (2012) Animal models of human pathology 2012. *J. Biomed. Biotechnol. 2012*, 404130.
(28) Li, Z., Zhao, G., Qian, S., Yang, Z., Chen, X., Chen, J., Cai, C., Liang, X., and Guo, J. (2012) Cerebrovascular protection of β-asarone in Alzheimer's disease rats: A behavioral, cerebral blood flow, biochemical and genic study. *J. Ethnopharmacol. 144*, 305−312.
(29) Cohen, A. S., Dubikovskaya, E. A., Rush, J. S., and Bertozzi, C. R. (2010) Real-time bioluminescence imaging of glycans on live cells. *J. Am. Chem. Soc. 132*, 8563−8565.
(30) Neves, A. A., Stöckmann, H., Harmston, R. R., Pryor, H. J., Alam, I. S., Ireland-Zecchini, H., Lewis, D. Y., Lyons, S. K., Leeper, F. J., and Brindle, K. M. (2011) Imaging sialylated tumor cell glycans in vivo. *FASEB J. 25*, 2528−2537.
(31) van Berkel, S. S., van Eldijk, M. B., and van Hest, J. C. (2011) Staudinger ligation as a method for bioconjugation. *Angew. Chem., Int. Ed. 50*, 8806−8827.
(32) White, E. H., McCapra, F., and Field, G. F. (1963) The structure and synthesis of firefly luciferin. *J. Am. Chem. Soc. 85*, 337−343.
(33) Nguyen, D. P., Elliott, T., Holt, M., Muir, T. W., and Chin, J. W. (2011) Genetically encoded 1,2-aminothiols facilitate rapid and site-specific protein labeling via a bio-orthogonal cyanobenzothiazole condensation. *J. Am. Chem. Soc. 133*, 11418−11421.
(34) Ren, H., Xiao, F., Zhan, K., Kim, Y., Xie, H., Xia, Z., and Rao, J. (2009) A biocompatible condensation reaction for the labeling of terminal cysteine residues on proteins. *Angew. Chem., Int. Ed. 48*, 9658−9662.
(35) Ye, D., Liang, G., Ma, M. L., and Rao, J. (2011) Controlling intracellular macrocyclization for the imaging of protease activity. *Angew. Chem., Int. Ed. 50*, 2275−2279.
(36) Liang, G., Ren, H., and Rao, J. (2010) A biocompatible condensation reaction for controlled assembly of nanostructures in living cells. *J. Nat. Chem. 2*, 54−60.
(37) Prescher, J. A., and Contag, C. H. (2010) Guided by the light: visualizing biomolecular processes in living animals with bioluminescence. *Curr. Opin. Chem. Biol. 14*, 80−89.
(38) McCaffrey, A., Kay, M. A., and Contag, C. H. (2003) Advancing molecular therapies through in vivo bioluminescent imaging. *Mol. Imaging 2*, 75−86.
(39) Massoud, T. F., and Gambhir, S. S. (2003) Molecular imaging in living subjects: seeing fundamental biological processes in a new light. *Genes Dev. 17*, 545−580.
(40) Geiger, G. A., Parker, S. E., Beothy, A. P., Tucker, J. A., Mullins, M. C., and Kao, G. D. (2006) Zebrafish as a "biosensor"? Effects of ionizing radiation and amifostine on embryonic viability and development. *Cancer Res. 66*, 8172−8181.
(41) Henkin, A. H., Cohen, A. S., Dubikovskaya, E. A., Park, H. M., Nikitin, G. F., Auzias, M. G., Kazantzis, M., Bertozzi, C. R., and Stahl, A. (2012) Real-time noninvasive imaging of fatty acid uptake in vivo. *ACS Chem. Biol. 7*, 1884−1891.
(42) van de Bittner, G. C., Dubikovskaya, E. A., Bertozzi, C. R., and Chang, C. J. (2010) In vivo imaging of hydrogen peroxide production in a murine tumor model with a chemoselective bioluminescent reporter. *Proc. Natl. Acad. Sci. U.S.A. 107*, 21316−21321.
(43) Wehrman, T. S., Degenfeld, von, G., Krutzik, P. O., Nolan, G. P., and Blau, H. M. (2006) Luminescent imaging of beta-galactosidase activity in living subjects using sequential reporter-enzyme luminescence. *Nat. Methods 3*, 295−301.
(44) Scabini, M., Stellari, F., Cappella, P., Rizzitano, S., Texido, G., and Pesenti, E. (2011) In vivo imaging of early stage apoptosis by measuring real-time caspase-3/7 activation. *Apoptosis 16*, 198−207.
(45) Hickson, J., Ackler, S., Klaubert, D., Bouska, J., Ellis, P., Foster, K., Oleksijew, A., Rodriguez, L., Schlessinger, S., Wang, B., and Frost, D. (2010) Noninvasive molecular imaging of apoptosis in vivo using a modified firefly luciferase substrate, Z-DEVD-aminoluciferin. *Cell Death Differ. 17*, 1003−1010.
(46) Shah, K., Tung, C., Breakefield, X. O., and Weissleder, R. (2005) In vivo imaging of S-TRAIL-mediated tumor regression and apoptosis. *Mol. Ther. 11*, 926−931.
(47) Cosby, N., Scurria, M., Daily, W., and Ugo, T., Promega Corp., and Promega Biosciences Inc. (2007) Custom enzyme substrates for luciferase-based assays, *Cell Notes 18*, 9−11.
(48) Biserni, A.; Martorana, F.; Roncoroni, C.; Klaubert, D.; Maggi, A.; Ciana, P. (2010) Identification of apoptotic cells in reporter mice using modified luciferin, Promega Corporation Web site. http://www.promega.com/resources/articles/pubhub/identification-of-apoptotic-cells-in-reporter-mice-using-modified-luciferin. Accessed November 2012.
(49) Dragulescu-Andrasi, A., Liang, G., and Rao, J. (2009) In vivo bioluminescence imaging of furin activity in breast cancer cells using bioluminogenic substrates. *Bioconjugate Chem. 20*, 1660−1666.
(50) Yao, H., So, M., and Rao, J. (2007) A bioluminogenic substrate for in vivo imaging of beta-lactamase activity. *Angew. Chem., Int. Ed. 46*, 7031−7034.
(51) Goun, E. A., Pillow, T. H., Jones, L. R., Rothbard, J. B., and Wender, P. A. (2006) Molecular transporters: synthesis of oligoguanidinium transporters and their application to drug delivery and real-time imaging. *ChemBioChem 7*, 1497−1515.

(52) Reddy, G. R., Thompson, W. C., and Miller, S. C. (2010) Robust light emission from cyclic alkylaminoluciferin substrates for firefly luciferase. *J. Am. Chem. Soc. 132*, 13586−13587.
(53) Harwood, K. R., Mofford, D. M., Reddy, G. R., and Miller, S. C. (2011) Identification of mutant firefly luciferases that efficiently utilize aminoluciferins. *Chem. Biol. 18*, 1649−1657.
(54) Conley, N. R., Dragulescu-Andrasi, A., Rao, J., and Moerner, W. E. (2012) A selenium analogue of firefly d-luciferin with red-shifted bioluminescence emission. *Angew. Chem., Int. Ed. 51*, 3350−3353.
(55) McCutcheon, D. C., Paley, M. A., Steinhardt, R. C., and Prescher, J. A. (2012) Expedient synthesis of electronically modified luciferins for bioluminescence imaging. *J. Am. Chem. Soc. 134*, 7604−7607.
(56) O'Brien, M. A., Daily, W. J., Hesselberth, P. E., Moravec, R. A., Scurria, M. A., Klaubert, D. H., Bulleit, R. F., and Wood, K. V. (2005) Homogeneous, bioluminescent protease assays: caspase-3 as a model. *J. Biomol. Screening 10*, 137−148.
(57) Woodroofe, C. C., Shultz, J. W., Wood, M. G., Osterman, J., Cali, J. J., Daily, W. J., Meisenheimer, P. L., and Klaubert, D. H. (2008) N-Alkylated 6′-aminoluciferins are bioluminescent substrates for Ultra-Glo and QuantiLum luciferase: new potential scaffolds for bioluminescent assays. *Biochemistry 47*, 10383−10393.
(58) Jones, L. R., Goun, E. A., Shinde, R., Rothbard, J. B., Contag, C. H., and Wender, P. A. (2006) Releasable luciferin-transporter conjugates: tools for the real-time analysis of cellular uptake and release. *J. Am. Chem. Soc. 128*, 6526−6527.
(59) White, E. H., Wörther, H., Seliger, H. H., and MacElroy, W. D. (1966) Amino analogs of firefly luciferin and biological activity thereof. *J. Am. Chem. Soc. 9*, 2015−2019.
(60) White, E. H., Steinmetz, M. G., Miano, J. D., Wildes, P. D., and Morland, R. (1980) Chemi- and bioluminescence of firefly luciferin. *J. Am. Chem. Soc. 9*, 3199−3208.
(61) McLaughlin, J. N., Patterson, M. M., and Malik, A. B. (2007) Protease-activated receptor-3 (PAR3) regulates PAR1 signaling by receptor dimerization. *Proc. Natl. Acad. Sci. U.S.A. 104*, 5662−5667.
(62) Ito, K., Nishimura, W., Maeda, M., Gomi, K., Inouye, S., and Arakawa, H. (2007) Highly sensitive and rapid tandem bioluminescent immunoassay using aequorin labeled Fab fragment and biotinylated firefly luciferase. *Anal. Chim. Acta 588*, 245−251.
(63) Denmeade, S. R., Lou, W., Lövgren, J., Malm, J., Lilja, H., and Isaacs, J. T. (1997) Specific and efficient peptide substrates for assaying the proteolytic activity of prostate-specific antigen. *Cancer Res. 57*, 4924−4930.
(64) Monsees, T., Miska, W., and Geiger, R. (1994) Synthesis and characterization of a bioluminogenic substrate for alpha-chymotrypsin. *Anal. Biochem. 221*, 329−334.
(65) Oballa, R. M., Truchon, J., Bayly, C. I., Chauret, N., Day, S., Crane, S., and Berthelette, C. (2007) A generally applicable method for assessing the electrophilicity and reactivity of diverse nitrile-containing compounds. *Bioorg. Med. Chem. Lett. 17*, 998−1002.
(66) Da Silva, L. P., and Da Silva, J. C. (2011) Kinetics of inhibition of firefly luciferase by dehydroluciferyl-coenzyme A, dehydroluciferin and L-luciferin. *Photochem. Photobiol. Sci. 10*, 1039−1045.
(67) McBean, G. J., and Flynn, J. (2001) Molecular mechanisms of cystine transport. *Biochem. Soc. Trans. 29*, 717−722.
(68) Knickelbein, R. G., Seres, T., Lam, G., Johnston, R. B., and Warshaw, J. B. (1997) Characterization of multiple cysteine and cystine transporters in rat alveolar type II cells. *Am. J. Physiol. 273*, L1147−1155.
(69) Chen, Z., Fei, Y.-J., Anderson, C. M. H., Wake, K. A., Miyauchi, S., Huang, W., Thwaites, D. T., and Ganapathy, V. (2003) Structure, function and immunolocalization of a proton-coupled amino acid transporter (hPAT1) in the human intestinal cell line Caco-2. *J. Physiol. 546*, 349−361.
(70) Shikano, N., Nakajima, S., Kotani, T., Ogura, M., Sagara, J., Iwamura, Y., Yoshimoto, M., Kubota, N., Ishikawa, N., and Kawai, K. (2007) Transport of d-[1−14C]-amino acids into Chinese hamster ovary (CHO-K1) cells: implications for use of labeled d-amino acids as molecular imaging agents. *Nucl. Med. Biol. 34*, 659−665.
(71) www.taconic.com.
(72) Cao, Y., Wagers, A. J., Beilhack, A., Dusich, J., Bachmann, M. H., Negrin, R. S., Weissman, I. L., and Contag, C. H. (2004) Shifting foci of hematopoiesis during reconstitution from single stem cells. *Proc. Natl. Acad. Sci. U.S.A. 101*, 221−226.
(73) Gross, S., and Piwnica-Worms, D. (2005) Real-time imaging of ligand-induced IKK activation in intact cells and in living mice. *Nat. Methods 2*, 607−614.
(74) Contag, C. H., Spilman, S. D., Contag, P. R., Oshiro, M., Eames, B., Dennery, P., Stevenson, D. K., and Benaron, D. A. (1997) Visualizing gene expression in living mammals using a bioluminescent reporter. *Photochem. Photobiol. 66*, 523−531.
(75) Shinde, R., Perkins, J., and Contag, C. H. (2006) Luciferin derivatives for enhanced in vitro and in vivo bioluminescence assays. *Biochemistry 45*, 11103−11112.
(76) Chandran, S. S., Williams, S. A., and Denmeade, S. R. (2009) Extended-release PEG-luciferin allows for long-term imaging of firefly luciferase activity in vivo. *Luminescence 24*, 35−38.
(77) Vieira, J., Da Silva, L. P., and Da Silva, J. C. (2012) Advances in the knowledge of light emission by firefly luciferin and oxyluciferin. *Photochem. Photobiol., B 117C*, 33−39.
(78) Kelkar, M., and de Abhijit. (2012) Bioluminescence based in vivo screening technologies. *Curr. Opin. Pharmacol. 12*, 592−600.
(79) Welsh, D. K., and Noguchi, T. (2012) Cellular bioluminescence imaging. *Cold Spring Harbor Protoc. 2012*, 852−866.
(80) Kim, S. B. (2012) Labor-effective manipulation of marine and beetle luciferases for bioassays. *Protein Eng., Des. Sel. 25*, 261−269.
(81) Zinn, K. R., Chaudhuri, T. R., Szafran, A. A., O'Quinn, D., Weaver, C., Dugger, K., Lamar, D., Kesterson, R. A., Wang, X., and Frank, S. J. (2008) Noninvasive bioluminescence imaging in small animals. *ILAR J. 49*, 103−115.
(82) Chaudhari, A. J., Darvas, F., Bading, J. R., Moats, R. A., Conti, P. S., Smith, D. J., Cherry, S. R., and Leahy, R. M. (2005) Hyperspectral and multispectral bioluminescence optical tomography for small animal imaging. *Phys. Med. Biol. 50*, 5421−5441.
(83) Liu, J. J., Wang, W., Dicker, D. T., and El-Deiry, W. S. (2005) Bioluminescent imaging of TRAIL-induced apoptosis through detection of caspase activation following cleavage of DEVD-amino-luciferin. *Cancer Biol. Ther 4*, 885−892.
(84) Ray, P., de Abhijit, Patel, M., and Gambhir, S. S. (2008) Monitoring caspase-3 activation with a multimodality imaging sensor in living subjects. *Clin. Cancer Res. 14*, 5801−5809.
(85) Laxman, B., Hall, D. E., Bhojani, M. S., Hamstra, D. A., Chenevert, T. L., Ross, B. D., and Rehemtulla, A. (2002) Noninvasive real-time imaging of apoptosis. *Proc. Natl. Acad. Sci. U.S.A. 99*, 16551−16555.
(86) Zhou, W., Shultz, J. W., Murphy, N., Hawkins, E. M., Bernad, L., Good, T., Moothart, L., Frackman, S., Klaubert, D. H., Bulleit, R. F., and Wood, K. V. (2006) Electrophilic aromatic substituted luciferins as bioluminescent probes for glutathione S-transferase assays. *Chem. Commun.*, 4620−4622.
(87) Zhou, W., Valley, M. P., Shultz, J., Hawkins, E. M., Bernad, L., Good, T., Good, D., Riss, T. L., Klaubert, D. H., and Wood, K. V. (2006) New bioluminogenic substrates for monoamine oxidase assays. *J. Am. Chem. Soc. 128*, 3122−3123.
(88) Cali, J. J., Ma, D., Sobol, M., Simpson, D. J., Frackman, S., Good, T. D., Daily, W. J., and Liu, D. (2006) Luminogenic cytochrome P450 assays. *Expert Opin. Drug Metab. Toxicol. 2*, 629−645.
(89) Wilson, J. W., Schurr, M. J., LeBlanc, C. L., Ramamurthy, R., Buchanan, K. L., and Nickerson, C. A. (2002) Mechanisms of bacterial pathogenicity. *Postgrad. Med. J. 78*, 216−224.
(90) Merrifield, R. B., and Stewart, J. M. (1965) Automated peptide synthesis. *Nature 207*, 522−523.
(91) Merrifield, R. B. (1965) Automated synthesis of peptides. *Science 150*, 178−185.
(92) Liang, Y., Walczak, P., and Bulte, J. W. (2012) Comparison of red-shifted firefly luciferase Ppy RE9 and conventional Luc2 as bioluminescence imaging reporter genes for in vivo imaging of stem cells. *J. Biomed. Opt 17*, 016004.

(93) Keyaerts, M., Caveliers, V., and Lahoutte, T. (2012) Bioluminescence imaging: looking beyond the light. *Trends Mol. Med. 18*, 164−172.
(94) Badr, C. E., and Tannous, B. A. (2011) Bioluminescence imaging: progress and applications. *Trends Biotechnol. 29*, 624−633.
(95) Razgulin, A., Ma, N., and Rao, J. (2011) Strategies for in vivo imaging of enzyme activity: an overview and recent advances. *Chem. Soc. Rev. 40*, 4186−4216.
(96) Miyashita, T., Okamura-Oho, Y., Mito, Y., Nagafuchi, S., and Yamada, M. (1997) Dentatorubral pallidoluysian atrophy (DRPLA) protein is cleaved by caspase-3 during apoptosis. *J. Biol. Chem. 272*, 29238−29242.
(97) Shin, S., Sung, B. J., Cho, Y. S., Kim, H. J., Ha, N. C., Hwang, J. I., Chung, C. W., Jung, Y. K., and Oh, B. H. (2001) An anti-apoptotic protein human survivin is a direct inhibitor of caspase-3 and -7. *Biochemistry 40*, 1117−1123.
(98) Jurisicova, A., Antenos, M., Varmuza, S., Tilly, J. L., and Casper, R. F. (2003) Expression of apoptosis-related genes during human preimplantation embryo development: potential roles for the Harakiri gene product and Caspase-3 in blastomere fragmentation. *Mol. Hum. Reprod. 9*, 133−141.
(99) Lakhani, S. A., Masud, A., Kuida, K., Porter, G. A., Booth, C. J., Mehal, W. Z., Inayat, I., and Flavell, R. A. (2006) Caspases 3 and 7: key mediators of mitochondrial events of apoptosis. *Science 311*, 847−851.
(100) Estaquier, J., Vallette, F., Vayssiere, J., and Mignotte, B. (2012) The mitochondrial pathways of apoptosis. *Adv. Exp. Med. Biol. 942*, 157−183.
(101) Donahue, B. S., Gailani, D., Higgins, M. S., Drinkwater, D. C., and George, A. L. (2003) Factor V Leiden protects against blood loss and transfusion after cardiac surgery. *Circulation 107*, 1003−1008.
(102) Angelillo-Scherrer, A., AdeFrutos, P., Aparicio, C., Melis, E., Savi, P., Lupu, F., Arnout, J., Dewerchin, M., Hoylaerts, M., Herbert, J., Collen, D., Dahlbäck, B., and Carmeliet, P. (2001) Deficiency or inhibition of Gas6 causes platelet dysfunction and protects mice against thrombosis. *Nat. Med. 7*, 215−221.
(103) van Berkel, S. S., van der Lee, B., van Delft, F. L., Wagenvoord, R., Hemker, H. C., and Rutjes, F. P. (2012) Fluorogenic peptide-based substrates for monitoring thrombin activity. *ChemMedChem 7*, 606−617.
(104) Seife, C. (1997) BIOMEDICINE: Blunting Nature's Swiss Army Knife. *Science 277*, 1602−1603.
(105) Go, R. S., and Adjei, A. A. (1999) Review of the comparative pharmacology and clinical activity of cisplatin and carboplatin. *J. Clin. Oncol. 17*, 409−422.
(106) Sleijfer, D. T., Meijer, S., and Mulder, N. H. (1885) Cisplatin: a review of clinical applications and renal toxicity. *Pharm. World Sci. 7*, 237−244.
(107) Lyseng-Williamson, K. A., and Fenton, C. (2005) Docetaxel: a review of its use in metastatic breast cancer. *Drugs 65*, 2513−2531.
(108) Diéras, V. (1997) Review of docetaxel/doxorubicin combination in metastatic breast cancer. *Oncology 11*, 31−33.
(109) Fulton, B., and Spencer, C. M. (1996) Docetaxel. A review of its pharmacodynamic and pharmacokinetic properties and therapeutic efficacy in the management of metastatic breast cancer. *Drugs 51*, 1075−1092.
(110) Michael, A., Syrigos, K., and Pandha, H. (2009) Prostate cancer chemotherapy in the era of targeted therapy. *Prostate Cancer Prostatic Dis. 12*, 13−16.
(111) Halder, J., Landen, C. N., Lutgendorf, S. K., Li, Y., Jennings, N. B., Fan, D., Nelkin, G. M., Schmandt, R., Schaller, M. D., and Sood, A. K. (2005) Focal adhesion kinase silencing augments docetaxel-mediated apoptosis in ovarian cancer cells. *Clin. Cancer Res. 11*, 8829−8836.
(112) Stennicke, H. R., and Salvesen, G. S. (1999) Caspases: preparation and characterization. *Methods 17*, 313−319.